Title

Assessment of tensile residual stress mitigation in Alloy 22 welds due to laser peening

Journal

Journal of Engineering Materials and Technology-Transactions of the ASME, 126(4)

ISSN

0094-4289

Authors

DeWald, A T
Rankin, J E
Hill, Michael R
et al.

Publication Date

2004-10-01

Peer reviewed

Adrian T. DeWald
Department of Mechanical and Aeronautical Engineering,
University of California,
One Shields Avenue,
Davis, CA 95616
Laser Science and Technology,
Lawrence Livermore National Laboratory,
PO Box 808, Livermore, CA 94550

Jon E. Rankin
Laser Science and Technology,
Lawrence Livermore National Laboratory,
PO Box 808, Livermore, CA 94550

Michael R. Hill*
e-mail address: mrhill@ucdavis.edu
Department of Mechanical and Aeronautical Engineering,
University of California,
One Shields Avenue,
Davis, CA 95616

Matthew J. Lee

Hao-Lin Chen

Laser Science and Technology,
Lawrence Livermore National Laboratory,
PO Box 808, Livermore, CA 94550

Assessment of Tensile Residual Stress Mitigation in Alloy 22 Welds Due to Laser Peening

This paper examines the effects of laser peening on Alloy 22 (UNS N06022), which is the proposed material for use as the outer layer on the spent-fuel nuclear waste canisters to be stored at Yucca Mountain. Stress corrosion cracking (SCC) is a primary concern in the design of these canisters because tensile residual stresses will be left behind by the closure weld. Alloy 22 is a nickel-based stainless steel that is particularly resistant to corrosion, however, there is a chance that stress corrosion cracking could develop given the right environmental conditions. Laser peening is an emerging surface treatment technology that has been identified as an effective tool for mitigating tensile redisual stresses in the storage canisters. The results of laser-peening experiments on Alloy 22 base material and a sample 33 mm thick double-V groove butt-weld made with gas tungsten arc welding (GTAW) are presented. Residual stress profiles were measured in Alloy 22 base material using the slitting method (also known as the crack-compliance method), and a full 2D map of longitudinal residual stress was measured in the sample welds using the contour method. Laser peening was found to produce compressive residual stress to a depth of 3.8 mm in 20 mm thick base material coupons. The depth of compressive residual stress was found to have a significant dependence on the number of peening layers and a slight dependence on the level of irradiance. Additionally, laser peening produced compressive residual stresses to a depth of 4.3 mm in the 33 mm thick weld at the center of the weld bead where high levels of tensile stress were initially present. [DOI: 10.1115/1.1789957]

1 Introduction

The U.S. Department of Energy (DOE) has been charged with developing a facility for the safe storage of spent nuclear material in a centralized location [1]. This effort has been named the Yucca Mountain Project (YMP) after the proposed site in the Nevada desert where the material will be stored. The goal of this project is to design a repository that will isolate hazardous nuclear waste from the environment for thousands of years [2]. The combination of the extremely long design life and the high consequence of failure presents unique engineering challenges and has required particularly careful study of every possible failure mode.

A highly corrosion-resistant material, Alloy 22 (UNS N06022) [3], will be used for the outer layer of the waste package to minimize the possibility of failure due to corrosive environmental conditions. After being loaded with radioactive material, the cylindrical canisters will be sealed with a final closure weld, which will leave behind a tensile residual stress from welding. One of the most studied failure mechanisms for the waste package system is stress corrosion cracking (SCC). For SCC to occur, three conditions must exist simultaneously. These conditions are a susceptible material, a corrosive environment, and a state of tensile stress. Since Alloy 22 has been shown in recent studies to be vulnerable to SCC under extreme conditions (acidic solution, elevated temperature, and weld residual stresses) [4], and the second condition cannot be controlled with absolute certainty, it is necessary to eliminate the tensile residual stresses in the waste-package welds. Laser peening is one of a few candidate technologies being examined as a method to mitigate tensile residual stresses and reduce the possibility for SCC.

Laser peening is an emerging surface-treatment technology that was developed in the 1970s at Battelle Columbus Laboratories [5–11], but its entrance to the commercial marketplace has been protracted due to limitations in laser technology. Like other similar surface treatments, laser peening is used to generate a compressive stress on the surface of a part that has been shown to inhibit failures caused by failure mechanisms, including fatigue and SCC [12]. While other surface treatment techniques, such as shot peening, are only capable of producing compressive stress down to depths of a few tenths of a millimeter [13], depths of compressive residual stress for laser-peened components are typically on the order of 1 or 2 mm [14]. In this work, depths of up to and beyond 4 mm are demonstrated, which is important in the design of the canisters because compressive surface stresses must remain as the outer layer of the canister becomes thinner over time due to general corrosion [3].

Surface preparation is necessary prior to laser peening. First, a protective layer is applied to the surface; this is called the ablative layer because its surface is ablated off during treatment. Typical ablative layer materials include opaque tape or paint [15]. Next, a transparent inertial tamping layer is applied over the ablative layer, which acts to confine the expansion of the high-pressure plasma to be generated by a laser pulse [16] (Fig. 1). Typical materials for the confinement layer include water and glass [17]. After these two surface layers are in place, the laser peening process can be carried out.

Laser peening uses a pulsed, high-power laser to generate high-

*Corresponding author.

Contributed by the Materials Division for publication in the JOURNAL OF ENGINEERING MATERIALS AND TECHNOLOGY. Manuscript received by the Materials Division July 21, 2003; revision received February 26, 2004. Associate Editor: S. Mall.

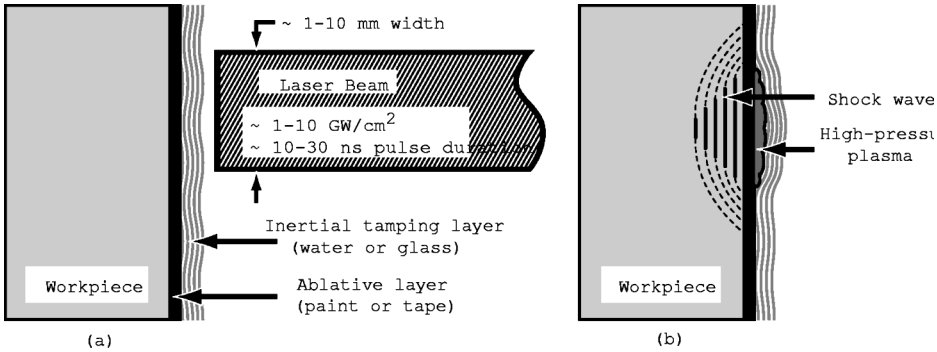

Fig. 1 Description of laser-peening process: (a) workpiece is covered with a protective ablative layer and an inertial confinement layer, a pulsed, high-energy laser is fired at the part, and (b) a region of high-pressure plasma is generated, which causes a shock wave to travel through the material.

pressure plasma on a small region of the part surface. The laser is fired at the material and the photons in the laser beam pass through the transparent tamping layer and are absorbed by the opaque ablative layer, which forms a high-pressure plasma. The expansion of the plasma is confined by the inertial tamping layer, causing a significant pressure to develop on the surface of the part. The duration of the laser pulse is on the order of 20 ns, and the short duration pressure pulse causes a shock wave to travel through the material that leaves plastically deformed material in its wake. The deformed material must remain in geometric compatibility with the bulk material, and an equilibrium state is obtained with the laser-peened area in a state of compressive residual stress. Laser peening is applied in a spot by spot manner with typical spot dimensions ranging from around 1 mm on a side [18] up to 1 centimeter [14], with spot shapes being round or rectangular. Multiple layers of laser peening are commonly used to help ensure that there is uniform coverage and to increase the depth of the compressive residual stress [19,20]. A layer of laser peening refers to a nominal 100% coverage of the treatment area with a slight overlap between successive spots. In most cases the ablative layer is replaced between peening layers.

There are significant absolute requirements on the specifications of the laser used for laser peening. The laser must be capable of producing an irradiance (power per unit area) on the order of $1-10$ GW/cm^2 (dependent on Hugonoit elastic limit of the treated material) with a pulse duration on the order of 10–30 ns. In addition to these requirements, it is also highly desirable, from a practicality standpoint, that the laser system has a high energy per laser pulse and a high repetition rate (high average power). These parameters are important because they directly influence the total processing time for a given part. In general, an ideal irradiance and pulse duration are identified for a given material, which means that a laser with a higher total energy per pulse will be able to operate at the ideal irradiance and pulse duration with a larger spot size, reducing the total number of spots necessary to cover the prescribed peening area. Furthermore, a higher repetition rate will allow for rapid application of successive laser spots leading to an additional decrease in the total processing time. The requirements, along with the desirable parameters, vastly limit the number of capable laser-peening systems in existence.

The laser-peening treatment for this study was applied at Lawrence Livermore National Laboratory (LLNL). The laser system employed at LLNL is capable of generating up to 20 J of energy at a repetition rate of 6 Hz [21], which means that an area of approximately 0.17 m^2 can be covered per hour at an irradiance of 10 GW/cm^2 and a pulse duration of 25 ns. The laser system at LLNL also includes a stimulated Brillouin scattering (SBS) phase conjugation device, which provides uniform wavefront control [22]. The SBS ensures that a uniform energy distribution exists within the laser spot, which allows the laser to run at a high repetition rate without damaging the optics.

Previous studies have shown that the pulse duration, irradiance, and number of peening layers are the parameters that have the most significant impact on the residual stress introduced by laser peening [19]. The first objective of this paper is to summarize a brief parametric study of the effect of these parameters on the residual stress state generated in small Alloy 22 specimens. The complete parametric study is still in progress, but some of the important preliminary results are presented in this paper. The second objective of this study is to demonstrate the effect of laser peening on the residual stress in a thick Alloy 22 butt-welded plate. Residual stress measurements were made using mechanical release methods (slitting method [23,24] and contour method [25]) after problems were encountered using diffraction methods.

2 Methods

Laser-Peening Parameters for Alloy 22. The amount of published information regarding the effects of various laser-peening parameters on the residual stress generated in a specific material is very limited considering that the technology has existed for more than 30 years. The few published accounts that are available focus on materials commonly subjected to cyclic loading in fatigue-limited applications, such as titanium [20] and aluminum [14]. When an application arises requiring the treatment of an unconventional material like Alloy 22, the peening parameters are selected using a combination of published literature regarding similar materials, experience, and parametric studies in small coupons of base material. As stated above, previous research suggests that the pulse duration, irradiance, and the number of layers have the most significant impact on the residual stress developed by laser peening. Experiments have shown that the plastically affected depth is controlled by the pulse duration [26], with a long pulse inducing a greater depth of compressive residual stress, and by the number of peening layers, with more layers producing deeper compressive residual stress [19].

A parametric study investigating the effect of the number of peening layers and the irradiance on the residual stress state generated in Alloy 22 was performed. Residual stress measurements were made on small blocks peened with a varying number of layers (2, 4, 10, and 20) at constant irradiance and pulse duration, and small blocks peened with a varying irradiance (7, 10, and 13 GW/cm^2) at a constant number of layers and pulse duration. In each case a nominally square shaped laser spot was used with a side length of approximately 3.0 mm. Each laser spot overlapped its neighbors by 10% of the spot length in both directions. A

Table 1 Specimen matrix for laser peening parameter study

Specimen number	Irradiance (GW/cm^2)	Number of layers	Pulse duration (ns)
07-10	7	10	25
10-10	10	10	25
13-10	13	10	25
10-02	10	2	25
10-04	10	4	25
10-20	10	20	25

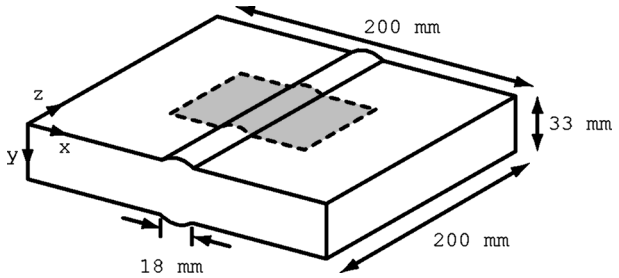

Fig. 2 Geometry of 33 mm thick butt-weld specimen (laser-peened area shaded)

summary of the parametric study is presented in Table 1. An additional residual stress measurement was performed on an unpeened specimen to determine the amount of residual stress present in the blocks prior to laser peening.

The in-plane dimensions of the Alloy 22 blocks used for the parametric study were 38×38 mm and the thickness was 20 mm. The blocks were removed from unused sections of a butt-welded plate using a wire electric discharge machine (EDM). The laser peening was applied in a rectangular pattern that covered roughly 30×30 mm of the top surface with a pattern of 11×11 spots. The blocks were peened using an ablative layer of 120 μm thick aluminum tape (replaced between layers) and a tamping layer of approximately 1 mm thick flowing water.

The residual stress in the blocks was measured using the slitting method (also known as the crack-compliance method), which was first published by Vaidyanathan and Finnie in 1971 [23] and recently reviewed by Prime [24]. This method uses metallic foil strain gages to measure the strain released during incremental cuts into the depth of the material. The recorded strain versus depth data are used to solve for the initial residual stress normal to the plane of the cut through elastic inverse methods [27].

The residual stress was measured as a function of the depth at the middle of the top surface. On the laser-peened blocks, foil strain gages with a grid length of 0.787 mm were applied to the top surface roughly 2.54 mm from the location of the cut and on the back surface directly below the center of the cut. A layer of silicone was applied over the strain gages to protect them from moisture during the experiment. The cutting was performed on a wire EDM with 0.25 mm diameter brass wire in increments of 0.13 mm to a total depth of 1.02 mm, 0.25 mm to a total depth of 2.54 mm, 0.51 mm to a total depth of 8.64 mm, and 1.02 mm to a final depth of 18.80 mm. Released strain was read with a commercial Wheatstone bridge instrument and recorded by hand after each slitting increment. Precise measurements of the position of the strain gages relative to the position of the cut were made after the completion of the experiment using photogrammetry. A similar procedure was followed for the unpeened block except that smaller depth increments were used due to the expected shallow depth of residual stress (increments of 0.025 mm to a total depth of 0.25 mm, 0.051 mm to a total depth of 0.51 mm, 0.076 mm to a total depth of 0.90 mm, 0.102 mm to a total depth of 1.40 mm, 0.127 mm to a total depth of 2.30 mm, and 0.25 mm thereafter). For a more thorough description of the theory and application of the slitting method please consult Refs. [24] and [27].

In order to select the best set of laser-peening parameters for Alloy 22, an objective system of judging the residual stress profiles is required. The primary figure of merit for this laser-peening application is the depth where the tensile residual stress reaches 20% of the material yield strength ($S_y=372$ MPa for Alloy 22 heat treated plate, 20% $S_y=74.4$ MPa), which was identified by YMP personnel as the level of tensile residual stress significant to their life prediction calculations. The secondary figures of merit for this application are the depth of compressive residual stress (zero stress crossing) and the magnitude of near-surface residual stress. For quantitative comparison, the near-surface residual stress was determined at 0.15 mm below the surface, which was a near-surface value where results were available for all measurements. The slitting results will be summarized based on these figures of merit.

Residual Stress Determination in Peened and Unpeened Alloy 22 Welds. Residual stress was also determined in as-welded and laser-peened sections of a quality-controlled 33 mm thick welded plate. This weld was an Alloy 22, multipass, double-V groove, butt-welded (GTAW) plate prepared by a commercial provider. The original welded plate had a length of 812 mm and a width of 200 mm. The plate was cut into four nominally identical 200 mm long sections, two of which were used for this experiment (Fig. 2). Since the plate was made by continuous welding, it is assumed that the weld residual stress in each specimen is similar. Therefore, measuring the residual stress in two specimens, one with and one without laser peening, will demonstrate the effect of laser peening on the welded plate.

One of the sample weld specimens was laser peened at LLNL. Peening was performed with a pulse duration of 25 ns, an irradiance of 10 GW/cm^2, and 10 peening layers. These parameters were selected before the completion of the parametric study due to the accelerated schedule under which this effort was performed. Laser peening was applied to a region at the center of the specimen, measuring 100 mm in the transverse direction and 76 mm in the longitudinal direction (Fig. 2).

The longitudinal component of residual stress in the peened and unpeened weld specimens was measured using the recently developed contour method [25]. An illustrative description of the contour method will be given in two dimensions (for simplicity), but the measurement principle applies equally in three dimensions. The principle behind the contour method is that when a part containing residual stress is cut in half along a straight line [Fig. 3(*a*)] the newly created free surface will deform as the stresses normal to the surface are released by cutting [Fig. 3(*b*)]. The deformations of the cut surface can be used to uniquely determine the initial residual stress acting normal to the cut plane using Bueckner's superposition principle [Fig. 3(*c*)] provided the stress release was elastic. The contour method, therefore, consists of three steps: 1) cutting of the part at the location where residual stress is to be determined, 2) measurement of the cut surface profile, and 3) calculation of the precut residual stress.

From an experimental standpoint, one must cut the part in half with a very controlled method that does not significantly alter the existing residual stress field (wire EDM typical). The cut for this measurement was performed on a submerged wire EDM with 0.25 mm diameter brass wire and finish cut settings to minimize the roughness along the surface of the cut. The specimen was securely clamped to a thick aluminum backing plate during the cutting process to minimize the amount that the part was able to move as residual stresses were released. The clamping helps to satisfy two assumptions made during the contour analysis: that the stress release is elastic (as clamping reduces stress concentration at the cut tip), and that the plane of the cut does not grossly deviate from a straight line.

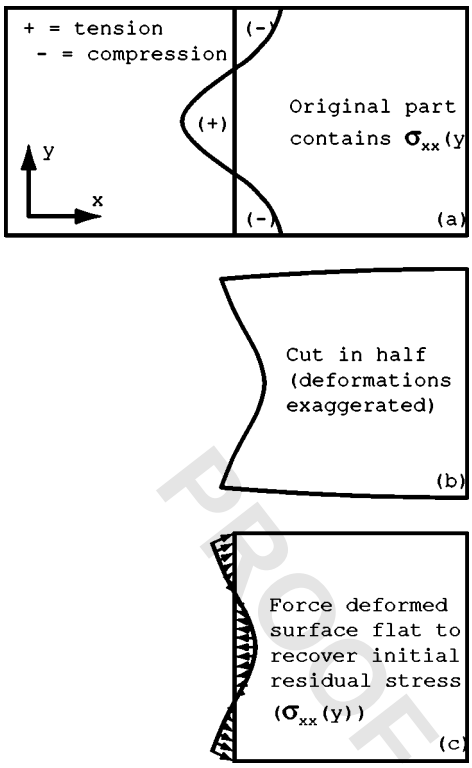

Fig. 3 Contour method principle: (*a*) a body containing unknown residual stress is cut in half, (*b*) the free surface deforms as the stresses normal to the plane of the cut are released, and (*c*) applying the opposite of the deformations back to the part recovers the initial residual stress state.

The measurement of the cut surfaces was performed at LLNL using a high-precision coordinate measuring machine (CMM) running in drag mode (i.e., the CMM probe remains in contact with the part as it moves across the surface taking data at specified increments, in contrast with pecking mode where the probe is lifted off between each measurement). A 2.0 mm diameter silicon nitride tip was used for the measurements, which limits the impact of surface roughness on the data since the large diameter ball contacts only the high points of the rough EDM surface. Both halves of the cut were measured with a point spacing of approximately 0.5 mm in the transverse and depth directions (x and y directions on Fig. 2) over the entire cut surface. A region consisting of about 30 mm to either side of the weld center was measured with a point spacing of 0.25 mm to better capture the surface profile in the area of expected stress gradients. The point spacing described above resulted in approximately 25,800 data points for each of the two surfaces. The deformations from opposite sides of the cut were averaged to remove anti-symmetric effects of shear stresses present along the plane of the cut and nonlinearities in the cutting path [25].

A finite element model of the part was used to convert the measured deformations back to residual stress. Since the surface deformations are small (typically on the order of tens of microns) it is equivalent to apply the inverse of the measured surface to an initially flat surface or to flatten a surface that contains the measured contour. From a practicality standpoint, however, it is much simpler to generate a model with an initially flat surface [25].

Surface profile data were numerically reduced, and reduced data were fit to a smooth surface to eliminate surface roughness effects. The data from each surface were first translated and rotated until they were aligned with the same coordinate system. To ensure that measurements were made near the edges of the surface, each CMM line scan was started and completed off the edge of the surface so that the edge would be explicitly apparent when the data were examined. Since data were collected beyond the coupon edges, the data set had to be filtered to remove points that were not actually part of the surface. Since the cross section of the surface was not perfectly rectangular, simply trimming points with a rectangular mask was not a viable option. An effective method for systematically removing the data points that were not part of the surface was developed. This method operated only on data within 8.0 mm of the surface perimeter, dividing it up into 20 small patches (each roughly 20 mm$\times$8 mm), and then individually fitting the patches with a first-order Fourier surface (nine terms). All of the data points that were not within 7 μm of this fitted surface were then removed, and the remaining data were again fit to a first-order Fourier surface. This process of fitting the small patches of data and removing points continued until no points remained that were outside the specified 7 μm tolerance from the surface fit. Once the data from off the edges were removed, the deformed surfaces from each half of the cut were individually fit to a Fourier surface to smooth out the influence of surface roughness. For both coupons, a sixth-order Fourier surface (169 terms) was used because this order was sufficient to produce a plateau in the root mean square (RMS) error between the data and the fit. The two Fourier surfaces were then interpolated at a set of common locations (finite element node locations), and the two data sets were averaged to get the average surface deformation due to residual stress release.

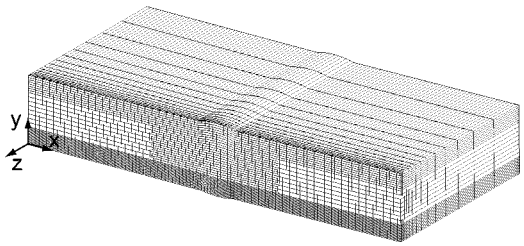

Fig. 4 Finite element model of half of the sample weld specimen

A finite element model of half of the weld specimen was generated consisting of 55,560 eight-node, linear brick elements with incompatible modes for enhanced bending performance. The model was made to represent the geometry of the welded plate after it has been cut in half (Fig. 4). The number of elements on the top surface and throughout the middle of the surface was increased to allow for better spatial resolution of the resulting residual stress field and to help ensure that the solution was converged. The mesh on the bottom surface is even more refined to get additional spatial resolution within the peened region. The negative of the deformed contour from the average surface was applied to the finite element model as a displacement boundary condition at nodal locations on the cut surface of the finite element model. An equilibrium step was taken, and the resulting stress normal to the surface was calculated, which is the estimate of residual stress prior to sectioning.

The results from the finite element model provide the residual stress acting normal to the plane of the cut over the entire cut surface. A contour plot of residual stress over the weld cross section is an effective way to visualize the resulting residual stress. Contour plots of residual stress were prepared for both the as-welded and laser-peened specimens to show how laser peening affects the residual stress. While the contour plot is helpful in visualizing the results, it is difficult to draw any quantitative conclusions about the effects of laser peening from a contour plot. For this reason, line plots of the residual stress versus depth from the surface were prepared for both specimens at three different locations [center of weld bead (x=102 mm), weld bead toe (x=111 mm), outside of weld (x=132 mm)].

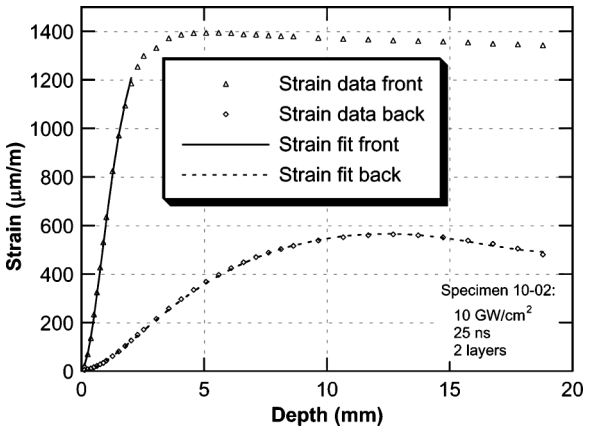

Fig. 5 Experimentally measured strain data and strain fit for specimen 10-02

In order to investigate the repeatability of the contour method, the difference between the residual stress in the as-welded and laser-peened specimens was also examined. The residual stress in the laser-peened specimen should be the superposition of the residual stress in the as-welded specimen, a change in the residual stress field near the peened surface due to laser-peening-induced plasticity, and a planar stress field (axial plus bending) developed to satisfy force and moment equilibrium on the cross section. Therefore, the results of the two measurements should differ by a nonplanar amount near the surface (laser-peening-affected region) and a planar amount below the plastically affected depth. Line plots of the difference in residual stress between the two measurements were prepared at the three locations where line plots of stress versus depth were also prepared.

3 Results

Laser-Peening Parameter Variations. To help the reader gain an understanding of the data reduction for the slitting experiments, an example of the experimentally measured strains and the elastic inverse solution strain fit is shown in Fig. 5 (specimen 10-02). Notice that the fit lines for the two strain gages, which result from a single fit, match up well with the experimental data. This reduces the amount of uncertainty in the calculated residual stresses. Additionally, Fig. 5 illustrates why it is important to have gages on both the front and back surfaces of the specimen. For shallow cut depths, the front gage shows good measurement sensitivity, but eventually the strain readings on the front gage plateau and yield no further useful information. As the front-gage sensitivity decreases, the back-gage sensitivity increases and provides useful information for the remainder of the experiment. In the data-reduction scheme employed here, data that was recorded from the front gage after it lost sensitivity was removed before the fitting took place. In the case of specimen 10-02, only the first 12 readings from the front gage were included. This is illustrated in Fig. 5 as the point where the front gage fit line stops.

Plots of residual stress versus depth from the surface for the laser-peening parameter study are shown in Fig. 6, and the figures of merit for each specimen are summarized in Table 2. Figure 6(*a*) displays the effect of the number of layers (2, 4, 10, and 20 layers) on the residual stress state, and Fig. 6(*b*) displays the effect of irradiance (7, 10, 13 GW/cm^2) on the residual stress state. The results show that there is a clear increase in the depth of residual stress (both 20% S_y crossing and zero crossing) when multiple layers are added up to 4, but it is difficult to establish a clear trend after this point. Additionally, it appears as though the levels of irradiance examined in this study produce only a slight amount of variation on the figures of merit (Table 2). This suggests that deviations from the desired level of irradiance due to variations in

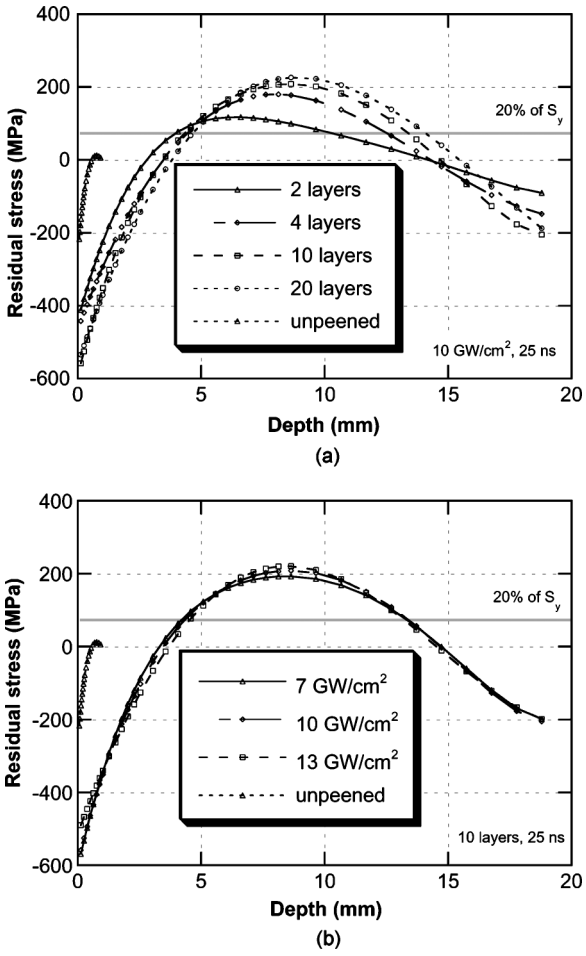

Fig. 6 Residual stress versus depth for laser peening parameter study: (*a*) effect of number of layers on residual stress state and (*b*) effect of irradiance on residual stress state

the laser energy of a given pulse will not significantly affect the residual stress state as long as they are within the range examined in this study (7 – 13 GW/cm^2). The residual stress in the unpeened block is shown up to a depth of 1 mm (Fig. 6); residual stresses beyond this depth were insignificant. The magnitude and depth of residual stress in the untreated blocks is small compared those present after laser peening.

Laser-Peened and As-Welded Plates. The data reduction for the contour method is relatively simple to visualize. The remaining data points, after filtering of near-edge data, were fit to a smooth surface. In the present work each data set was fit to a Fourier surface, the surfaces were interpolated at common points (finite element node locations), and the two interpolated surfaces were averaged. The progression of the data reduction from raw

Table 2 Summary of figures of merit for each laser-peening parametric study specimen

Specimen number	Depth of 20% S_y crossing (mm)	Depth of zero crossing (mm)	Magnitude of near surface stress (MPa)
07-10	4.2	3.3	−550
10-10	4.4	3.5	−560
13-10	4.6	3.7	−490
10-02	4.0	2.8	−410
10-04	4.5	3.5	−440
10-20	4.7	3.8	−540

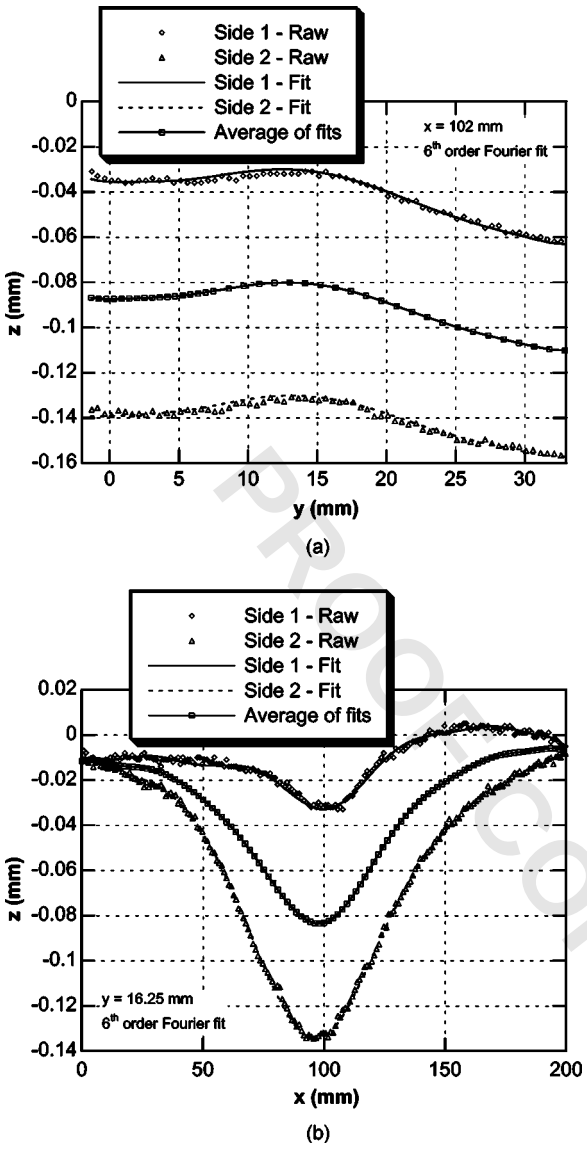

Fig. 7 Sample of a measured surface line trace from each half of the cut (as-welded specimen) with fits to each surface shown along with the average of both fits: (*a*) line trace along $x=102$ mm and (*b*) line trace along $y=16.25$ mm

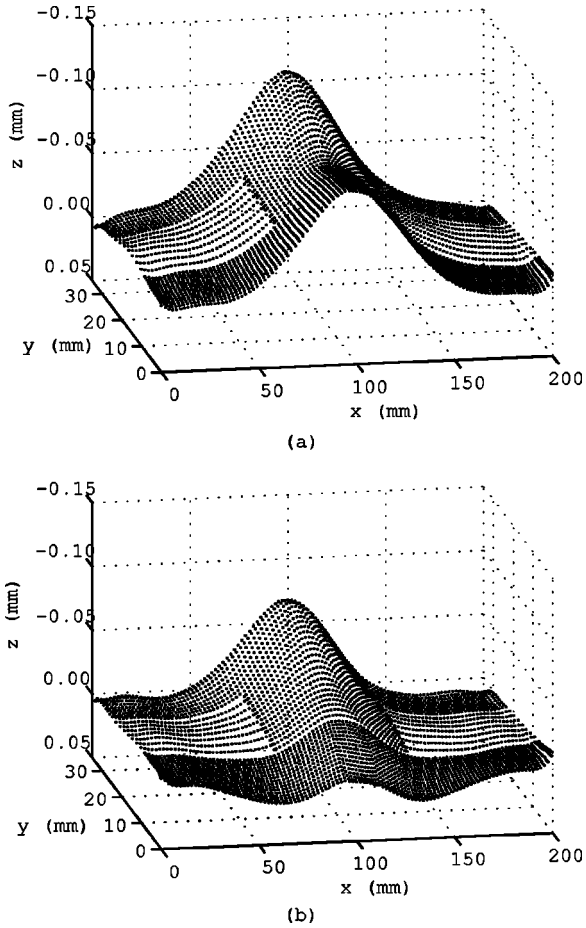

Fig. 8 Final CMM surface (after fitting, and averaging) interpolated at finite element node locations and inverted (for clarity): (*a*) as-welded weld and (*b*) laser-peened weld (laser peening applied along *y*-min surface from $x=50$ to $x=150$)

data, to fitted data, to averaged data is shown in Fig. 7 for lines of constant x and y taken from the middle of the data for the as-welded specimen ($x=102$ mm, $y=16.25$ mm). Note that the data may contain an arbitrary rigid-body rotation, which will not affect the computed stresses [25]. Additionally, the difference in magnitude of surface displacement from one side of the cut to the other is caused by either the initial presence of shear stresses on the cut-plane or cut-path wandering [25]. The data reduction is illustrated with line plots because they allow for easy visualization of the progression without the complications of 3D graphing. The actual data reduction involved surfaces rather than lines, but the same procedure was used.

The final CMM surfaces, after fitting, interpolation at finite element node locations, and averaging, are shown in Figs. 8(*a*) (as-welded) and 8(*b*) (peened). The z axis on the plots is reversed to allow for better visualization of the data. The peak to valley range of the displacements is 116 μm for the as-welded specimen and 92 μm for the peened specimen, which is large compared to the accuracy of the measurement device (± 1 μm). The differences between the surface displacements for the as-welded and laser-peened weld are easily distinguishable, and these lead to significant differences in the computed residual stress. Note that laser peening was applied along the y-min surface of Fig. 8(*b*) between $x=50$ mm and $x=150$ mm.

The resulting residual stress distribution for the peened and as-welded specimens are shown as contour plots in Fig. 9. Notice that laser peening produces a deep layer of uniform compressive stress throughout the entire treated region [bottom edge of Fig. 9(*b*)]. The peak levels of tensile residual stress are redistributed toward the center of the thickness where they will not negatively affect the material's vulnerability to SCC.

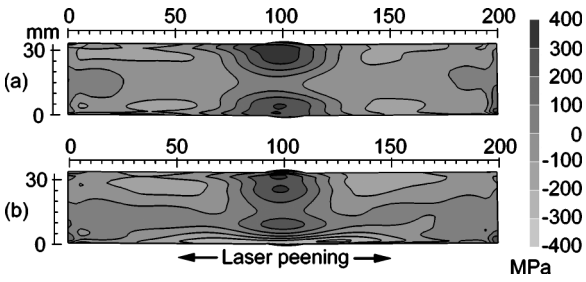

Fig. 9 Contour plot of residual stress distribution across the plane of the sample weld: (*a*) before laser peening treatment and (*b*) after laser-peening treatment on bottom surface

PROOF COPY 007404JYT

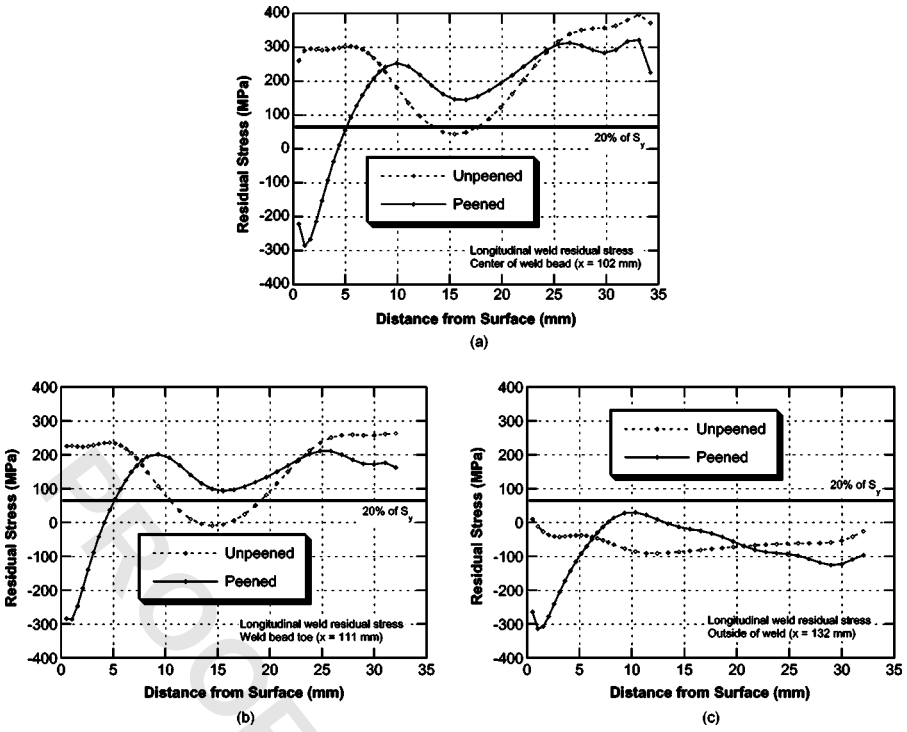

Fig. 10 Line plots of residual stress and distribution before and after laser-peening treatment: (a) center of weld bead, (b) weld bead toe (9 mm from center), and (c) outside of weld (30 mm from center)

In order to allow for quantitative comparison between the peened and the as-welded specimen, line plots of residual stress versus depth from the bottom surface are shown for the center of the weld bead ($x = 102$ mm), the weld toe ($x = 111$ mm), and outside the weld region ($x = 132$ mm) (Fig. 10). These plots show that laser peening is very effective in eliminating near surface tensile residual stresses that were left behind by the welding process. At each location, laser peening transformed a tensile or near zero surface stress into a compressive residual stress down to a depth of at least 4.3 mm (center of weld bead) and up to 7.7 mm (30 mm from weld center). Additionally, the depth of 20% yield crossing is 5.3 mm for the worst case (center of weld bead and weld bead toe).

Subtracting the residual stress in the laser-peened weld from the residual stress in the untreated weld gives the change in residual stress caused by laser peening (Fig. 11). As previously stated, the change in residual stress should consist of a nonplanar distribution within the laser-peening affected zone plus a planar component elsewhere. The linearity of the change in residual stress outside the laser-peened region serves to illustrate the repeatability of the contour method. Figure 11 also shows that in this experiment, laser peening plastically affected material down to a depth of roughly 11 mm.

4 Discussion

The two objectives of this work were to summarize a parametric study of the effect of the number of peening layers and the laser pulse irradiance on the residual stress generated in Alloy 22 and to determine the effect of laser peening on the longitudinal component of residual stress in a thick Alloy 22 butt-welded plate. Throughout this study a few choices were made in selecting methods, and the consequences of these choices will be discussed in the following paragraphs.

One of the most fundamental methodological decisions made during this experiment was the selection of a residual stress-measurement technique capable of providing data for comparison of process variations. Previous work has obtained good results using x-ray diffraction (XRD) to measure residual stress profiles in laser-peened specimens [14,20]. While XRD is a valuable tool for measuring near-surface residual stress, it is difficult to use this technique to measure stresses far from the surface. Additionally, measurements showed that the average grain size for similarly prepared Alloy 22 material varied from approximately 50 to 150 μm for a group of specimens. Materials with grains of this size or larger have been known to cause experimental difficulties for diffraction measurements [28]. Early in the test program, an attempt was made to measure the residual stress to a depth of 4.0 mm in a set of 13.5 mm thick Alloy 22 specimens using XRD with layer removal. Three Alloy 22 specimens were peened with a varying number of layers (2, 4, and 10) at a laser setting of 10 GW/cm^2

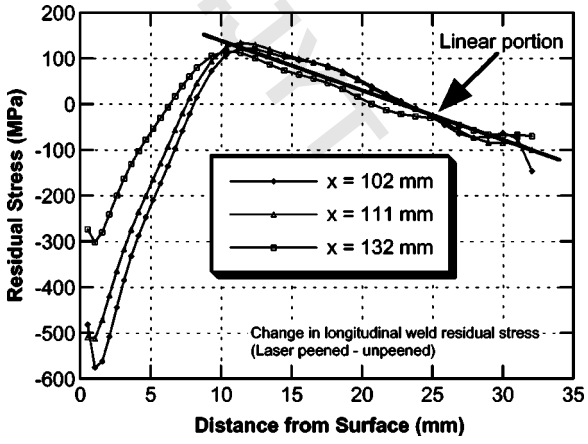

Fig. 11 Contour plot of the change in residual stress caused by laser peening [peened minus as-welded residual stress from Fig. 9(*a*) through Fig. 9(*c*)]

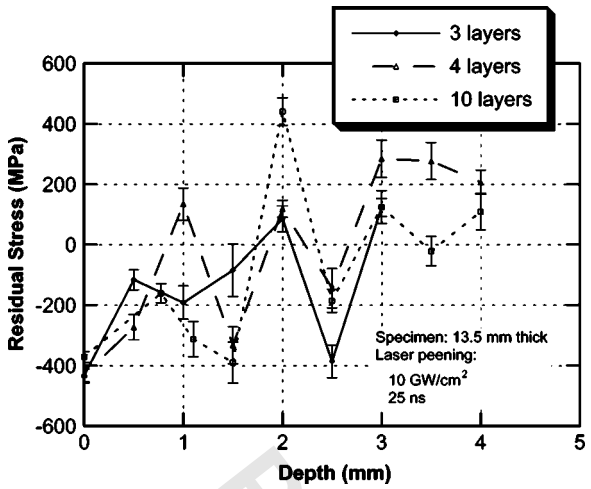

Fig. 12 Effect of number of peening layers on residual stress in 13.5 mm thick Alloy 22 specimens measured using x-ray diffraction with layer removal

and 25 ns. The XRD work was performed by a commercial provider (with a record of obtaining good results in smaller grained materials) and the results are shown in Fig. 12. These results provide no basis for a determination of the effect of the number of layers of peening on the residual stress state, and therefore, XRD was deemed unsuitable for ranking one set of laser-peening parameters relative to another.

The slitting method is possibly the best method to measure residual stress through the thickness of small blocks of laser-peened material because of the strong signal that the foil strain gages can pick up for the given specimen geometry and residual stress distribution. One assumption of the slitting method that sometimes limits its applicability is that the stress is uniform along the length of the slit. In this work, laser peening was applied uniformly over the specimen surface, and this assumption is valid.

The contour method has recently emerged as a tool for mapping residual stresses in specimens with two-dimensional nonuniform residual stress variations. Welds are one of the more practical applications for this method because residual stresses are often an issue in their mechanical performance and the residual stresses are spatially nonuniform. Another method to measure a spatial distribution of residual stresses in welds is neutron diffraction. However, it is difficult to make these measurements in thick sections because they require long measurement times for spatially resolved results [29] and suitable facilities exist in only a few locations. In addition, there are troublesome issues with determining the stress-free lattice spacing inside the weld region due to microstructural variation from the welding process [29]. Although neutron diffraction is difficult and time-consuming in thick-welded joints, a number of such studies have been published in the literature (e.g., [29,30]). In contrast, the analysis for the contour method is only dependent on the elastic properties of the material that are not significantly affected by microstructure or grain-size variations, making the contour method well suited for measuring residual stresses in welds. Results of the contour method and neutron diffraction have been compared and were found to be in agreement in welded coupons [31].

The most significant aspect of the results presented here is the deep level of residual stress that is induced in Alloy 22 by laser peening. The depth of compressive residual stress measured here is up to 3.8 mm in 20 mm thick blocks and varied from 4.3 mm to 7.7 mm in a 33 mm thick weld. The depth of compressive residual stress is a function of both the depth of plastic deformation induced by laser peening and the geometric constraint of the peened geometry. For a given depth of laser-peening-induced plastic deformation, a thick geometry will exhibit deeper compressive residual stress than a thin geometry. This effect must be considered when estimating the depth of residual stress in a full-scale component from results in a test specimen of a different thickness and geometric constraint.

From the results presented here, it is difficult to give an answer as to what is the optimal (effective and efficient) set of laser-peening parameters for welds in Alloy 22 storage canisters. Current work is under way to cover a larger range of the number of layers (below 10 layers) and larger range of the irradiance (below 7 GW/cm^2). From the results presented in this paper it appears as though a peening treatment at 7 GW/cm^2 with 4 layers of peening will produce a satisfactory residual stress state with the least amount of effort. These peening parameters (7 GW/cm^2, 25 ns, and 4 layers) would lead to a 72% decrease in total peening time for the weld joint studied, compared to the parameters that were actually used (10 GW/cm^2, 25 ns, and 10 layers). This helps to illustrate that it is important to establish minimum values for both irradiance and the number of peening layers such that test samples, and the waste packages, can be peened in the least amount of time.

There are many specific benefits that can be realized by laser peening the Alloy 22 storage canisters. The most direct benefit is that laser peening significantly decreases the possibility for SCC to occur since it produces such a deep layer of compressive stress on the surface of the part. This depth is important because predicted general corrosion of Alloy 22 over the design life of these canisters will result in thinning of the cylinder wall [3]. The effect of thinning of the cylinder wall on the residual stress induced by laser peening is a topic of current research. Initial results suggest that the depth of compressive stress relative to the original surface will increase as material is removed from the outer surface of the cylinder because the depth of laser-peening-induced plasticity is greater than the original depth of compressive residual stress.

Another benefit of laser peening for this application is the potential to reduce the thickness of the Alloy 22 layer while maintaining the same level of safety. Since Alloy 22 is very expensive, and a great deal of this material will be required over the life of the project, any reduction in the amount of material would lead to a significant cost reduction for the project. Additionally, laser peening could open the door to using other materials instead of Alloy 22 for the storage canisters since there is the possibility that a less expensive stainless steel that has been laser peened will have similar stress corrosion-resistance properties to unpeened Alloy 22 material.

Laser peening is also advantageous from an applications standpoint. First, laser peening can be easily adapted to treat more complicated geometries. The energy for laser peening is delivered to the part in the form of photons, which are absorbed and produce high-pressure plasma. The pressure always applies a force normal to the surface and the magnitude of the pressure is constant for a given level of irradiance (regardless of the incidence angle of the photons, up to a limit of roughly 60 deg). Therefore, laser peening can effectively treat geometrically complex surfaces. There is evidence of this at the weld toe of the welded specimen in this study [Figs. 9(b) and 10(b)], where consistent levels of compressive residual stress exist despite the surface feature. Similar geometric features may pose difficulties for other surface treatment techniques. Further, the weld bead on this specimen is a small feature that does not fully demonstrate the capability to treat complex shapes, and laser peening is currently deployed in the treatment of more complex shapes, such as those of turbine engine components [20]. A second advantage of laser peening is related to the fixturing of treated parts. Since the pressure buildup during laser peening lasts for a short amount of time (less than 100 ns), the reaction force required to keep the part stationary is minimal because the fixture will experience only a small impulse, which can be largely attenuated by fixture compliance.

Acknowledgments

The authors greatly appreciate several contributions to this collaborative work. The authors would like to thank Mike Prime of Los Alamos National Laboratory for his helpful discussions related to the contour method. The laser peening treatment was applied at LLNL by Laurie Lane. Additional support was provided by personnel at LLNL including Lloyd Hackel, Bob Yamamoto, Steve Mills, and Frank Wong. For the contour measurement, the EDM cutting was performed by Mike Dean at Trisan Manufacturing, Inc., and the surface measurement was performed by Curt Garrett at LLNL. Funding for this research was provided by the Student Employee Graduate Research Fellowship at LLNL. This work was performed under the auspices of the U.S. Department of Energy by University of California, Lawrence Livermore National Laboratory under Contract No. W-7405-Eng-48.

References

[1] Bodvarsson, G. S., Boyle, W., Patterson, R., and Williams, D., 1999, ''Overview of Scientific Investigations at Yucca Mountain—The Potential Repository for High-Level Nuclear Waste,'' J. Containment Tech., **38**, pp. 3–24.

[2] Repository Safety Strategy: US Department of Energy's Strategy to Protect Public Health and Safety After Closure of a Yucca Mountain Repository, Revision 1, US Dept. of Energy, p. ■, 1998.

[3] Farmer, J., McCright, D., Gdowski, G., Wang, F., Summers, T., Bedrossian, P., Horn, J., Lian, T., Estill, J., Lingenfelter, A., and Halsey, W., 2000, ''General and Localized Corrosion of Outer Barrier of High-Level Waste Container in Yucca Mountain,'' *Transportation, Storage, and Disposal of Radioactive Materials Pressure Vessles and Piping*, Seattle, WA, R. S. Hafner, ed., ASME, Vol. 408, p. 53–70.

[4] Farmer, J., Lu, S., Summers, T., McCright, D., Lingenfelter, A., Wang, F., Estill, J., Hackel, L., Chen, H.-L., Gordon, G., Pasupathi, V., Andersen, P., Tang, S., and Herrera, M., 2000, ''Modeling and Mitigation of Stress Corrosion Cracking in Closure Welds of High-Level Waste Container for Yucca Mountain,'' *Transportation, Storage, and Disposal of Radioactive Materials Pressure Vessles and Piping*, Seattle, WA, R. S. Hafner, ed., ASME, Vol. 408, p. 71–81.

[5] Fairland, B. P., Wilcox, B. A., Gallagher, W. J., and Williams, D. N., 1972, ''Laser Shock-Induced Microstructural and Mechanical Property Changes in 7075 Aluminum,'' J. Appl. Phys., **43**(9), pp. 3893–3895.

[6] Fairand, B. P., Clauer, A. H., and Jung, R. G., 1974, ''Quantitative Assessment of Laser-Induced Stress Waves Generated at Confined Surface,'' Appl. Phys. Lett., **25**(8), pp. 431–433.

[7] Clauer, A. H., Fairand, B. P., and Wilcox, B. A., 1976, ''Laser Shock Hardening of Weld Zones in Aluminum Alloys,'' Metall. Trans. A, **8A**, pp. 1871–1876.

[8] Fairland, B. P., and Clauer, A. H., 1976, ''Use of Laser Generated Shocks to Improve the Properties of Metals and Alloys,'' Indust. Appli. High Power Laser Tech., **86**, pp. 112–119.

[9] Fairland, B. P., and Clauer, A. H., 1976, ''Effect of Water and Paint Coatings on the Magnitude of Laser-Generated Shocks,'' Opt. Commun., **18**(4), pp. 588–591.

[10] Clauer, A. H., Fairand, B. P., and Wilcox, B. A., 1977, ''Pulsed Laser Induced Deformation in an Fe-3 Wt Pct Si Alloy,'' Metall. Trans. A, **8A**, pp. 119–125.

[11] Fairand, B. P., and Clauer, A. H., 1979, ''Laser Generation of High Amplitude Stress Waves in Materials,'' J. Appl. Phys., **50**(3), pp. 1497–1502.

[12] Peyre, P., Braham, C., Ledion, J., Berthe, L., and Fabbro, R., 2000, ''Corrosion Reactivity of Laser-Peened Steel Surfaces,'' J. Mater. Eng. Perform., **9**(6), pp. 656–662.

[13] Zhuang, W. Z., and Halford, G. R., 2001, ''Investigation of residual stress relaxation under cyclic load,'' Int. J. Fatigue, **23**, pp. S31–S37.

[14] Peyre, P., Fabbro, R., Merrien, P., and Lieurade, H. P., 1996, ''Laser Shock Processing of Aluminum Alloys: Application to High Cycle Fatigue Behavior,'' Mater. Sci. Eng., A, **210**, pp. 102–113.

[15] Montross, C. S., Florea, V., and Swain, M. V., 2001, ''The Influence of Coatings on Subsurface Mechanical Properties of Laser Peened 2011-T3 Aluminum,'' J. Mater. Sci., **36**, pp. 1801–1807.

[16] Fabbro, R., Fournier, J., Ballard, P., Devaux, D., and Virmont, J., 1990, ''Physical Study of Laser-Produced Plasma in Confined Geometry,'' J. Appl. Phys., **68**(2), pp. 775–784.

[17] Devaux, D., Fabbro, R., Tollier, L., and Bartnicki, E., 1993, ''Generation of shock waves by laser-induced plasma in confined geometry,'' J. Appl. Phys., **74**(4), pp. 2268–2273.

[18] Schmidt-Uhlig, R., Karlitschek, P., Yoda, M., Sano, Y., and Marowsky, G., 2000, ''Laser Shock Processing With 20 MW Laser Pulses Delivered by Optical Fibers,'' Eur. Phys. J. A, **9**, pp. 235–238.

[19] Fabbro, R., Peyre, P., Berthe, L., and Scherpereel, X., 1998, ''Physics and Applications of Laser-shock Processing,'' J. Laser Appl., **10**(6), pp. 265–279.

[20] Smith, P. R., Shepard, M. J., Prevey, P. S., and Clauer, A. H., 2000, ''Effect of Power Density and Pulse Repetition on Laser Shock Peening of Ti-6Al-4V,'' J. Mater. Eng. Perform., **9**(1), pp. 33–37.

[21] Dane, C. B., Hackel, L. A., Daly, J., and Harrisson, J., 2000, ''High Power Laser for Peening of Metals Enabling Production Technology,'' Mater. Manuf. Processes, **15**(1), pp. 81–96.

[22] Dane, C. B., Zapata, L. E., Neuman, W. A., Norton, M. A., and Hackel, L. A., 1995, ''Design and Operation of a 150 W Near Diffraction-Limited Laser Amplifier With SBS Wavefront Correction,'' IEEE J. Quantum Electron., **31**(1), pp. 148–163.

[23] Vaidyanathan, S., and Finnie, I., 1971, ''Determination of Residual Stresses From Stress Intensity Factor Measurements,'' ASME J. Basic Eng., **93**, pp. 242–246.

[24] Prime, M. B., 1999, ''Residual Stress Measurement by Successive Extension of a Slot: The Crack Compliance Method,'' Appl. Mech. Rev., **52**(2), pp. 75–96.

[25] Prime, M. B., 2001, ''Cross-Sectional Mapping of Residual Stresses by Measuring the Surface Contour After a Cut,'' ASME J. Eng. Mater. Technol., **123**, pp. 162–168.

[26] Masse, J.-E., and Barreau, G., 1995, ''Laser Generation of Stress Waves in Metal,'' Surf. Coat. Technol., **70**(2–3), pp. 231–234.

[27] Hill, M. R., and Lin, W. Y., 2002, ''Residual stress measurement in a ceramic-metallic graded material,'' ASME J. Eng. Mater. Technol., **124**(2), pp. 185–191.

[28] J. Lu, ed., 1996, *Handbook of Measurement of Residual Stresses*, Prentice-Hall, Englewood Cliffs, NJ.

[29] Krawitz, A. D., and Winholtz, R. A., 1994, ''Use of Position-Dependent Stress-free Standards for Diffraction Stress Measurements,'' Mater. Sci. Eng., A, **185**, pp. 123–130.

[30] Lorentzen, T., and Ibsø, J. B., 1995, ''Neutron Diffraction Measurements of Residual Strains in Offshore Welds,'' Mater. Sci. Eng., A, **197**, pp. 209–214.

[31] Prime, M. B., Hughes, D. J., and Webster, P. J., 2001, ''Weld Application of a New Method for Cross-Sectional Residual Stress Mapping,'' 2001 SEM Annual Conf. on Experimental and Applied Mechanics, Portland, OR608-611.